Lanthanide-induced relaxation anisotropy

Elizaveta A. Suturina[a], Kevin Mason[b], Carlos F.G.C. Geraldes[c],
Nicholas F. Chilton[d], David Parker[b],* and Ilya Kuprov[a],*

a) School of Chemistry, University of Southampton, Highfield, Southampton, SO17 1BJ, United Kingdom.

b) Department of Chemistry, Durham University, South Road, Durham, DH1 3LE, United Kingdom.

c) Department of Life Sciences and Coimbra Chemistry Centre, Faculty of Science and Technology, University of Coimbra, Calçada Martim de Freitas, 3000-456 Coimbra, Portugal.

d) School of Chemistry, University of Manchester, Oxford Road, Manchester, M13 9PL, United Kingdom.

Abstract

Lanthanide ions accelerate nuclear spin relaxation by two primary mechanisms: dipolar and Curie. Both are commonly assumed to depend on the length of the lanthanide-nucleus vector, but not on its direction. Here we show experimentally that this is wrong – careful proton relaxation data analysis in a series of isostructural lanthanide complexes (Ln=Tb, Dy, Ho, Er, Tm, Yb) reveals angular dependence in both Curie and dipolar relaxation. The reasons are: (a) that magnetic susceptibility anisotropy can be of the same order of magnitude as the isotropic part (contradicting the unstated assumption in Guéron's theory of the Curie relaxation process), and (b) that zero-field splitting can be much stronger than the electron Zeeman interaction (Bloembergen's original theory of the lanthanide-induced dipolar relaxation process makes the opposite assumption). These factors go beyond the well researched cross-correlation effects; they alter the relaxation theory treatment and make strong angular dependencies appear in the nuclear spin relaxation rates. Those dependencies are impossible to ignore – this is now demonstrated both theoretically and experimentally, and suggests that a major revision is needed of the way lanthanide-induced relaxation data is used in structural biology.

This paper is dedicated to the memory of Professor Nicolaas Bloembergen.

1. Introduction

Despite their reputation for being difficult, unpaired electrons have many applications in nuclear magnetic resonance:[1] paramagnetic chemical shifts are used to refine metalloprotein structures,[2] paramagnetic relaxation enhancement (PRE) is a valuable source of ligand binding data and imaging contrast,[3,4] and the recent rebirth of dynamic nuclear polarisation[5] is starting to yield real clinical results in cancer diagnostics.[6,7] Chemical shifts originating from both isotropic (contact shift) and anisotropic (pseudocontact shift, PCS) parts of the magnetic susceptibility tensor are well understood.[2,8] However, paramagnetic relaxation enhancement models often ignore the effects associated with the magnetic anisotropy of the lanthanide tag.

Nuclear relaxation anisotropy effects described in this paper have been neglected for so long because magnetic resonance imaging (MRI) contrast agents traditionally contain magnetically isotropic ions like Gd^{3+}, which simply accelerate proton relaxation all around.[9] Likewise, most PRE experiments use Mn^{2+} and Gd^{3+} complexes with negligible magnetic anisotropy to maximize the volume affected by the tag and minimise PCS.[10] However, the recently introduced *property responsive* PARASHIFT contrast agents[11,12] use a different kind of contrast that requires strong magnetic anisotropy in the lanthanide.[13-15] In a PARASHIFT probe, a reporter group (*e.g.* ^tBu or CF_3) is engineered into the ligand coordinating the paramagnetic ion. The reporter spins must resonate far away from water and fat signals, and relax sufficiently quickly to permit rapid pulsing used in MRI – relaxation rates of 100-500 Hz are considered optimal.[16] Even more stringent design requirements occur in triple imaging studies that aim to provide information on tissue temperature and pH. In that approach, an anatomical image from the water signal is obtained simultaneously with images from pH and temperature probe resonances, which must be well separated in frequency (>20,000 Hz) and must relax at similar rates.[12] The current theories of chemical shift and relaxation do not allow such properties to be predicted with confidence – even the smallest structural changes caused by the solvent can interfere with the trends in the paramagnetic shift.[17] Progress has only been made by examining trends in the behaviour of well-defined series of complexes.[18-20]

This project started when we found[17,21] that pseudocontact shifts predicted by Bleaney's theory[22] did not fit our experimental data for an isostructural series of magnetically anisotropic lanthanide complexes (Ln=Tb, Dy, Ho, Er, Tm, Yb) with octadentate ligands based on triphosphinate derivatives of 1,4,7,10-tetraazacyclododecane. Nuclear spin relaxation rates could not be fitted by the standard Zeeman limit expressions[2,23-28] or explained by any known cross-correlations.[29-36] In particular, they appeared to have second *and fourth* spherical rank with respect to the electron-nuclear direction vector in the molecular frame of reference. The deviation from the commonly used relaxation theory expressions was significant, and would have been problematic in biomolecular structure refinement. The situation clearly called for a more detailed nuclear spin relaxation model.

We therefore present a systematic study of nuclear spin relaxation enhancement in an isostructural series of lanthanide complexes. We show experimentally that the commonly employed "$1/r^6$" expressions for paramagnetic relaxation[2,24-28,36-42] fail to describe the observed nuclear spin relaxation rates, and proceed to derive and discuss more nuanced dipolar and Curie relaxation theories that account for the effects of magnetic susceptibility anisotropy and – crucially – zero-field splitting.

2. Nuclear relaxation in lanthanide-nucleus systems

Nuclear spin relaxation in liquid-phase paramagnetic systems in the Zeeman limit is extensively researched and reviewed.[2,24-28,36-42] The dominant methods are Bloch-Redfield-Wangsness (BRW) theory[43-45] that treats spatial motion as an external stochastic process, and the Fokker-Planck equation that considers the spatial motion explicitly.[46-48] This section reviews the classical results obtained in the limit of strong Zeeman interaction and isotropic magnetic susceptibility, and then proceeds to derive the expressions that do not make those assumptions.

2.1 The limit of strong Zeeman interaction

For the nuclear relaxation induced by a rapidly relaxing lanthanide ion, the dominant paramagnetic relaxation mechanisms are dipolar and Curie.[2] Both originate from the electron-nuclear dipolar interaction, but the Curie mechanism is different in that the nucleus is interacting with the thermal average of the electron magnetisation ("Curie spin"). This interaction is modulated by molecular motion but not by electron spin dynamics;[26] the resulting interaction presents itself mathematically as chemical shielding.[36] The expressions used in hundreds of recent papers are:[2]

$$R_1^{dip} = \frac{2}{15}\left(\frac{\mu_0}{4\pi}\right)^2 \frac{\gamma_N^2 \mu_{eff}^2}{r^6}\left[3j\left(\omega_N, \tau_{R,T_{1E}}\right) + 6j\left(\omega_E + \omega_N, \tau_{R,T_{2E}}\right) + j\left(\omega_E - \omega_N, \tau_{R,T_{2E}}\right)\right]$$

$$R_2^{dip} = \frac{1}{15}\left(\frac{\mu_0}{4\pi}\right)^2 \frac{\gamma_N^2 \mu_{eff}^2}{r^6}\left[\begin{array}{l}4j\left(0, \tau_{R,T_{1E}}\right) + 3j\left(\omega_N, \tau_{R,T_{1E}}\right) + 6j\left(\omega_E, \tau_{R,T_{2E}}\right) + \\ +6j\left(\omega_E + \omega_N, \tau_{R,T_{2E}}\right) + j\left(\omega_E - \omega_N, \tau_{R,T_{2E}}\right)\end{array}\right]$$

$$R_1^{Curie} = \frac{6}{5}\left(\frac{\mu_0}{4\pi}\right)^2 \frac{\omega_N^2 \mu_{eff}^4}{\left(3kT\right)^2 r^6} j\left(\omega_N, \tau_R\right)$$

$$R_2^{Curie} = \frac{1}{5}\left(\frac{\mu_0}{4\pi}\right)^2 \frac{\omega_N^2 \mu_{eff}^4}{\left(3kT\right)^2 r^6}\left[4j\left(0, \tau_R\right) + 3j\left(\omega_N, \tau_R\right)\right]$$

(1)

with the following shorthands for the spectral power density function and the characteristic times:

$$j\left(\omega, \tau\right) = \frac{\tau}{1 + \omega^2 \tau^2}, \qquad \tau_{R,T_{1E}} = \left(\frac{1}{\tau_R} + \frac{1}{T_{1E}}\right)^{-1}, \qquad \tau_{R,T_{2E}} = \left(\frac{1}{\tau_R} + \frac{1}{T_{2E}}\right)^{-1} \qquad (2)$$

In these expressions, μ_0 is vacuum permeability, γ_N is the magnetogyric ratio of the nucleus, ω_N is the nuclear Zeeman frequency, ω_E is the electron Zeeman frequency, μ_{eff} is the effective magnetic moment of the electron, r is the electron-nuclear distance, τ_R is the second rank rotational correlation time of what is often assumed to be isotropic rotational diffusion, T_{1E} is the longitudinal electron relaxation time, and T_{2E} is the transverse electron relaxation time.

These expressions have apparently served the magnetic resonance community quite well, particularly in the structural biology of metalloproteins.[2,8,28,49,50] Detailed derivations are available in the literature cited above; the multitude of cross-correlations between all the anisotropies involved is also very well researched.[29-36] However, the obvious and glaring problem with Equations (1) and all associated cross-correlations is that the majority of commonly used lanthanide complexes and experimental conditions *are not actually in the Zeeman limit* – at any reasonable magnetic fields, the dominant interaction by far is the zero-field splitting (ZFS) caused by ligand field.[51-53]

2.2 The general setting

The most sophisticated current theories of nuclear relaxation in non-gadolinium lanthanide systems are two-tiered. At the femtosecond-scale "fast" tier, the total electron momentum Hamiltonian[54]

$$\hat{H}_E = \hat{H}_{Zeeman} + \hat{H}_{ZFS} \tag{3}$$

contains the Zeeman interaction term and the ZFS term. Both have stochastic time-dependent components that cause electron relaxation. The large amplitude of both terms[55] (much bigger than nuclear magnetic interactions) and the short time scale of the resulting electron relaxation (picoseconds) means that nuclear spin interactions are inconsequential for the dynamics of the electron momentum. Because ZFS can be stronger than the Zeeman interaction (100-1000 cm^{-1} *vs.* 1-10 cm^{-1} in common NMR fields[54,55]), the interaction representation transformation within relaxation theories must include the ZFS.[40,56,57] The resulting dynamics is seen from a distance as a time-dependent magnetic moment $\vec{\mu}_E(t)$. It has the average value $\vec{\mu}^{(eq)}$ described by a magnetic susceptibility tensor χ, and some dynamics $\vec{\mu}(t)$ around that average in each individual system:

$$\vec{\mu}_E(t) = \vec{\mu}^{(eq)} + \vec{\mu}(t), \qquad \vec{\mu}^{(eq)} = \chi \cdot \vec{B}/\mu_0 \tag{4}$$

The dynamics in $\vec{\mu}(t)$ are determined by the simultaneous action of Zeeman interaction and ZFS.[40,56,57] Since both interactions are modulated by ligand cage vibrations, the problem of calculating the explicit form of $\vec{\mu}(t)$ is exceedingly difficult.

At the second stage of the theory, $\vec{\mu}_E(t)$ enters the microsecond-scale "slow" tier, where the nuclear spin Hamiltonian contains it as an external time-dependent magnetic moment:

$$\hat{H}_N = -\gamma_N \hat{\vec{I}}^T \cdot (\mathbf{1} - \boldsymbol{\sigma}_0) \cdot \vec{B} - \gamma_N \mu_0 \hat{\vec{I}}^T \cdot \mathbf{D} \cdot \vec{\mu}_E(t) \tag{5}$$

where $\boldsymbol{\sigma}_0$ is the chemical shielding tensor provided by the local electronic structure around the nucleus, and $\mathbf{D}$ is the dipolar coupling matrix between the nucleus and the lanthanide. A point dipolar coupling model is sufficient outside the first coordination sphere:

$$\mathbf{D} = \frac{1}{4\pi} \left[3 \frac{\vec{r} \cdot \vec{r}^T}{r^5} - \frac{\mathbf{1}}{r^3} \right] \tag{6}$$

where $\vec{r}$ is the lanthanide-nucleus distance vector. It is convenient to split $\vec{\mu}_E(t)$ according to Equation (4) and to rearrange the Hamiltonian:

$$\hat{H}_N = -\gamma_N \hat{\vec{I}}^T \cdot (\mathbf{1} - \boldsymbol{\sigma}_0 + \mathbf{D} \cdot \chi) \cdot \vec{B} - \gamma_N \mu_0 \hat{\vec{I}}^T \cdot \mathbf{D} \cdot \vec{\mu}(t) \tag{7}$$

The contribution to the chemical shielding tensor from the lanthanide magnetic susceptibility is now apparent[2,27,28] – the $\mathbf{D} \cdot \chi$ term gives rise to the pseudocontact shift and the Curie relaxation mechanism.[26,36] It is convenient to define the full nuclear shielding tensor as follows:

$$\boldsymbol{\sigma} = \boldsymbol{\sigma}_0 - \mathbf{D} \cdot \chi \tag{8}$$

For the purposes of relaxation theory, the stochastic time dependence in $\boldsymbol{\sigma}_0$, χ and $\mathbf{D}$ comes from molecular rotation. All three tensors are tied to the molecular frame of reference, but the nuclear spin is quantised *along the external magnetic field*. In the lab frame, the Zeeman term in Equation (7) therefore transforms in the following way under a molecular rotation with a unitary matrix $\mathbf{R}$:

$$\hat{\vec{I}}^{\mathrm{T}} \cdot \left(\mathbf{1} - \boldsymbol{\sigma}\right) \cdot \vec{B} \quad \xrightarrow{\mathbf{R}} \quad \hat{\vec{I}}^{\mathrm{T}} \cdot \mathbf{R}\left(\mathbf{1} - \boldsymbol{\sigma}\right)\mathbf{R}^{\mathrm{T}} \cdot \vec{B} \tag{9}$$

However, as pointed out by Kowalewski[51-53] and Sharp,[40,56,57] the electron magnetic moment is quantised *in the molecular frame of reference* when ZFS is much stronger than the Zeeman interaction, as in the cases considered here. Therefore, the dipolar term in Equation (7) transforms as follows:

$$\hat{\vec{I}}^{\mathrm{T}} \cdot \mathbf{D} \cdot \vec{\mu}(t) \quad \xrightarrow{\mathbf{R}} \quad \hat{\vec{I}}^{\mathrm{T}} \cdot \mathbf{R}\mathbf{D}\mathbf{R}^{\mathrm{T}}\mathbf{R} \cdot \vec{\mu}(t) = \hat{\vec{I}}^{\mathrm{T}} \cdot \mathbf{R}\mathbf{D} \cdot \vec{\mu}(t) \tag{10}$$

The final nuclear spin Hamiltonian that enters the Bloch-Redfield-Wangsness relaxation theory at the "slow" tier of the problem therefore is:

$$\hat{H}_{\mathrm{N}} = -\gamma_{\mathrm{N}}\hat{\vec{I}}^{\mathrm{T}} \cdot \mathbf{R}\left(\mathbf{1} - \boldsymbol{\sigma}\right)\mathbf{R}^{\mathrm{T}} \cdot \vec{B} - \gamma_{\mathrm{N}}\mu_0\hat{\vec{I}}^{\mathrm{T}} \cdot \mathbf{R}\mathbf{D} \cdot \vec{\mu}(t) \tag{11}$$

An important point here is that the two terms in this Hamiltonian are statistically independent because the dynamics in $\vec{\mu}(t)$ are uncorrelated with the molecular rotation $\mathbf{R}(t)$. We can therefore perform relaxation theory treatment for the two terms separately.

2.3 Anisotropic contributions to the Curie mechanism

Guéron's original derivation[26] uses the dipolar path, but it is clear from Equation (8) that the Curie relaxation mechanism[23-25] may be viewed as belonging to the chemical shift anisotropy (CSA) family – the magnetic susceptibility centre shields the nearby nuclei; this shielding is anisotropic, and therefore causes relaxation.[58] This section contains an *ab initio* derivation using the CSA approach.

In the usual case of a vertical magnet, $\vec{B} = \begin{bmatrix} 0 & 0 & B_0 \end{bmatrix}$. As prescribed by BRW theory,[43-45] we will put the isotropic chemical shielding into $\hat{H}_0$, and its anisotropy into $\hat{H}_1$:

$$\hat{H}_{\mathrm{N}}(t) = -\gamma_{\mathrm{N}}\hat{\vec{I}}^{\mathrm{T}} \cdot \left(\mathbf{1} - \mathbf{R}\boldsymbol{\sigma}\mathbf{R}^{\mathrm{T}}\right) \cdot \vec{B} = \hat{H}_0 + \hat{H}_1(t)$$
$$\hat{H}_0 = \omega_{\mathrm{N}}\hat{I}_{\mathrm{Z}}, \qquad \hat{H}_1(t) = \sum_{l=1,2} \sum_{m,k=-l}^{l} \mathfrak{D}_{km}^{(l)}(t)\hat{Q}_{km}^{(l)} \tag{12}$$

In this expression, $\omega_{\mathrm{N}} = -\gamma_{\mathrm{N}}\left(1 - \sigma_{\mathrm{iso}}\right)B_0$ is the isotropic Zeeman frequency of the nucleus. The anisotropic part is expressed *via* Wigner D functions $\mathfrak{D}_{km}^{(l)}$ of molecular orientation. The irreducible spherical components of the Hamiltonian $\hat{Q}_{km}^{(l)}$ are defined in Section 2 of our paper dealing with this subject.[59] The reason for moving into this representation is that BRW theory is formulated in terms of correlation functions of scalar parameters of the Hamiltonian.[43-45] These scalar parameters are conveniently exposed in Equation (12). This notation also corresponds directly to the structure of the relaxation module of *Spinach*[59] and lends itself easily to automatic symbolic processing.[60]

The general form of the Bloch-Redfield-Wangsness relaxation superoperator $\hat{\hat{R}}$ for the case of rotationally modulated interactions is:[59,61]

$$\hat{\hat{R}} = -\sum_{lnkmpq} \int_0^\infty G_{kmpq}^{(ln)}(\tau)\hat{\hat{Q}}_{km}^{(l)}e^{-i\hat{H}_0\tau}\hat{\hat{Q}}_{pq}^{(n)\dagger}e^{i\hat{H}_0\tau}\,d\tau \tag{13}$$

where the rotational correlation functions $G_{kmpq}^{(ln)}(\tau)$ are trajectory averages of the products of differently timed Wigner D functions from Equation (12):

$$G_{kmpq}^{(ln)}(\tau) = \left\langle \mathfrak{D}_{km}^{(l)}(t)\mathfrak{D}_{pq}^{(n)*}(t+\tau) \right\rangle \tag{14}$$

We shall assume isotropic rotational diffusion for the systems in question (this was checked using HYDRONMR[62] in Section 3), in which case

$$G_{kmpq}^{(ln)}(\tau) = \frac{\delta_{ln}\delta_{kp}\delta_{mq}}{2l+1} e^{-l(l+1)D\tau} \tag{15}$$

where δ denotes Kronecker symbols. The characteristic decay time of the (usually dominant) second rank terms is called rotational correlation time:

$$\tau_R = \frac{1}{6D} \tag{16}$$

where D is the rotational diffusion coefficient. *Mathematica* worksheets implementing Equations (12)-(15) are included in the *Supplementary Information*. Automated symbolic processing[60] yields the following BRW theory expressions:

$$R_1^{\text{Curie+CSA}} = \frac{1}{2}\Lambda_\sigma^2\omega_N^2\frac{\tau_R}{1+9\omega_N^2\tau_R^2} + \frac{2}{15}\Delta_\sigma^2\omega_N^2\frac{\tau_R}{1+\omega_N^2\tau_R^2}$$

$$R_2^{\text{Curie+CSA}} = \frac{1}{4}\Lambda_\sigma^2\omega_N^2\frac{\tau_R}{1+9\omega_N^2\tau_R^2} + \frac{1}{45}\Delta_\sigma^2\omega_N^2\left(4\tau_R + \frac{3\tau_R}{1+\omega_N^2\tau_R^2}\right) \tag{17}$$

where Λ_σ^2 is the first rank invariant of the total chemical shielding tensor:

$$\Lambda_\sigma^2 = \left(\sigma_{XY}-\sigma_{YX}\right)^2 + \left(\sigma_{XZ}-\sigma_{ZX}\right)^2 + \left(\sigma_{YZ}-\sigma_{ZY}\right)^2 \tag{18}$$

and Δ_σ^2 is the second rank invariant:

$$\Delta_\sigma^2 = \sigma_{XX}^2 + \sigma_{YY}^2 + \sigma_{ZZ}^2 - \sigma_{XX}\sigma_{YY} - \sigma_{XX}\sigma_{ZZ} - \sigma_{YY}\sigma_{ZZ} +$$

$$+ \frac{3}{4}\left[\left(\sigma_{XY}+\sigma_{YX}\right)^2 + \left(\sigma_{XZ}+\sigma_{ZX}\right)^2 + \left(\sigma_{YZ}+\sigma_{ZY}\right)^2\right] \tag{19}$$

It now becomes clear that there are two reasons why the Curie relaxation rate expressions commonly used in the literature (Eq. 38-39 in a major review of this subject,[39] Eq. 14-15 in Guéron's original paper[26] and many others) did not predict the angle dependence in the nuclear relaxation rates. The first reason is that the paramagnetic shielding term actually has not one, but two components:

$$\mathbf{D}\cdot\boldsymbol{\chi} = \left[\mathbf{D}\cdot\chi_{\text{iso}} + \mathbf{D}\cdot\boldsymbol{\chi}_{\text{aniso}}\right] \tag{20}$$

corresponding to the isotropic and the anisotropic parts of the magnetic susceptibility tensor. Guéron[26] did not consider susceptibility anisotropy. The other reason is that the antisymmetric component of the chemical shielding tensor, usually ignored in diamagnetic systems due to its small amplitude,[63] is significant here – the product of two symmetric matrices is only symmetric when they commute, which is not the case for $\mathbf{D}$ and $\boldsymbol{\chi}_{\text{aniso}}$. We therefore have the antisymmetric term in the shielding tensor that is of the same order of magnitude as the symmetric term, and must therefore be included into the analysis of the nuclear relaxation.[58] This term was omitted by Guéron (Eq. 14-15 in his paper[26]), but later included by Fiat and Vega (Eq. 22-23 in their paper[37]). The advantage of Equations (17)-(19) over the equivalent expressions reported by Fiat and Vega is the direct use of the Cartesian form of all tensors involved. This avoids the well-documented ambiguities, numerical instabilities and singularities associated with eigenvalues and Euler angles,[64,65] particularly when the equations are fitted to experimental data, and when $\boldsymbol{\sigma}_0$ cannot be ignored.

The presence of the $\mathbf{D} \cdot \boldsymbol{\chi}_{\text{aniso}}$ term in the chemical shielding tensor means that *nuclear relaxation rates depend on the angles* between the eigenframe of the magnetic susceptibility tensor and the electron-nuclear direction (Figure 1). The dependence in Equation (20) has a second spherical rank. Once the squares are taken in Equations (18) and (19), spherical ranks up to fourth make an appearance. It is also clear from Equation (20) that the relaxation rate will appear to depend on the sign of the pseudocontact shift – we shall see an experimental confirmation for this below.

Figure 1. Schematic illustration of the anisotropy in the Curie relaxation rate with respect to the direction of the lanthanide-nucleus vector. The contours are XZ plane slices through relaxation rate isosurfaces of equal value. **Left:** low field limit with respect to nuclear Zeeman frequency and the rotational correlation time. **Right:** high field limit. **Green contours:** isotropic magnetic susceptibility tensor. **Red contours:** maximum easy-axis (prolate) anisotropy $\chi_{\text{ax}} = 3\chi_{\text{iso}}$. **Blue contours:** maximum easy-plane (oblate) anisotropy $\chi_{\text{ax}} = -3\chi_{\text{iso}}/2$.

Equations (17) would reduce to Equation (1) if the magnetic susceptibility tensor were isotropic, but this is *absolutely not the case* in our systems, or for most lanthanide systems, where $\chi_{\text{ax}} = \chi_{\parallel} - \chi_{\perp}$ can be of the same order of magnitude as χ_{iso}. In the case of a Tm^{3+} complex from our recent work,[21] χ_{iso} = 0.49 Å^3 and χ_{ax} = 0.39 Å^3. Nuclei at the axial position relative to the eigenframe of $\boldsymbol{\chi}$ relax faster in the case of easy-axis anisotropy. In the case of easy-plane anisotropy, their relaxation is slower compared to the isotropic magnetic susceptibility case. The relaxation rate for the nuclei at the equatorial position is the same for easy-axis and isotropic cases, but it becomes faster in the case of easy-plane anisotropy (Figure 1).

The shape of the relaxation profile also depends on the magnetic field – at low field, Λ_{σ}^2 and Δ_{σ}^2 components of the longitudinal Curie relaxation rate are comparable, and therefore the angular dependence has a shamrock shape (Figure 1, left). In the strong field limit, the difference in the denominators of the first rank and the second rank components in Equation (17) makes the contribution from Δ_{σ}^2 dominant. The result (Figure 1, right) is a prolate ellipsoid-like shape for easy-axis anisotropy, and oblate for easy-plane. The interplay of the first and the second rank components in Equation (17) also complicates the magnetic field dependence of Curie relaxation rates – the denominators now have different multiples of the nuclear Zeeman frequency.

2.5 Anisotropic contributions to the dipolar mechanism

The lanthanide-induced dipolar mechanism of nuclear relaxation has a complicated history.[66] The rates for the dipolar relaxation process in the Zeeman limit were derived by Solomon,[23] extended to

the case of an anisotropic *g*-tensor by Sternlicht,[67] and also updated by Koenig[68] to account for the possible difference between longitudinal and transverse relaxation rates of the electron; all three works only considered the symmetric part of the electron-nuclear interaction tensor. The asymmetry was considered by Nordio and Segre,[69] who did however miss the electron relaxation rate correction. The Florence group pointed out that the frequencies entering the spectral power density terms in the Solomon equation must be modified in the presence of strong ZFS,[70,71] and that the perturbative formalism itself is suspect:[70,72] *"it appears that the deviation from the Solomon behaviour … is dramatic even at the high fields of today's spectrometers"*.[73] Similar conclusions were reached by Kowalewski *et al.*, who pointed out that Solomon equation breaks down in the limit of low magnetic field[51,52] and extended the theory into the slow motion limit. Several specific cases were analysed and found to depend strongly on the ZFS.[71,74] The suspicions were taken to their logical conclusion by Florence and Stockholm groups[38,51-53,70,72] and later Sharp[40,56,57] – ZFS can be *much greater* than the Zeeman interaction even at high field, and in those cases the electron magnetic moment is quantised in the molecular frame of reference rather than the magnet frame. Only in the case of the Gd^{3+} is ZFS sufficiently small for an elegant and complete perturbative treatment of ZFS relaxation to be possible.[75] Other lanthanides are considerably harder – at the moment, there are at least three distinct families of nuclear spin relaxation theories that reproduce, fully or partially, the magnetic field dependence of the relaxation rates.[76] Here we demonstrate experimentally that strong ZFS also makes nuclear dipolar relaxation rates depend on the direction of the electron-nucleus vector in the molecular frame of reference in a way that is completely independent from any cross-correlations. On the theoretical side, the key contribution of this work to the rather voluminous prior art is that, for the angle dependence of the relaxation rates, our final expressions are small, general, and easy to use.

If $\vec{\mu}(t)$ is the fluctuating part of the electron magnetic dipole written in the molecular frame of reference, then the electron-nuclear dipolar interaction operator in the laboratory frame of reference can be specified by Equation (10), in which case the Hamiltonians are:

$$\hat{H}_0 = \omega_N \hat{I}_Z, \qquad \hat{H}_1(t) = -\gamma_N \mu_0 \hat{\vec{I}}^T \cdot \mathbf{R}(t) \mathbf{D} \cdot \vec{\mu}(t) \qquad (21)$$

where $\mathbf{R}(t)$ is the overall molecular rotation matrix and $\mathbf{D}$ is defined in Equation (6). Statistical properties of $\mathbf{R}(t)$ are well understood,[77] but those of $\vec{\mu}(t)$ are not readily available or easily predictable because the electron Hamiltonian in Equation (3) is modulated by molecular vibrations, libration of coordinated solvent and other mechanisms with complicated frequency spectra and unknown statistics[40,56,57,78,79] that will imprint themselves onto $\vec{\mu}(t)$. However, it is reasonable to assume is that $\vec{\mu}(t)$ is not statistically correlated with $\mathbf{R}(t)$.

From the point of view of the nuclear spin, the structure of the Hamiltonian in Equation (21) is quite simple – it is a coupling to an oscillating external field:

$$\hat{H}_0 = \omega_N \hat{I}_Z, \qquad \hat{H}_1(t) = a_X(t)\hat{I}_X + a_Y(t)\hat{I}_Y + a_Z(t)\hat{I}_Z,$$
$$\vec{a}(t) = -\gamma_N \mu_0 \mathbf{R}(t) \mathbf{D} \cdot \vec{\mu}(t), \qquad \left\|\hat{H}_1(t)\right\| \ll \left\|\hat{H}_0\right\| \qquad (22)$$

The corresponding relaxation rates are easily expressed in terms of autocorrelation functions (trajectory average is denoted here and below by angular brackets) of the components of $\vec{a}(t)$ – see the *Mathematica* worksheet in the Supplementary Information:

$$R_X = \int_0^\infty \left\langle a_Y(t)a_Y(t+\tau)\right\rangle e^{-i\omega_N\tau}d\tau + \int_0^\infty \left\langle a_Z(t)a_Z(t+\tau)\right\rangle d\tau$$

$$R_Y = \int_0^\infty \left\langle a_X(t)a_X(t+\tau)\right\rangle e^{-i\omega_N\tau}d\tau + \int_0^\infty \left\langle a_Z(t)a_Z(t+\tau)\right\rangle d\tau \qquad (23)$$

$$R_Z = \int_0^\infty \left\langle a_X(t)a_X(t+\tau)\right\rangle e^{-i\omega_N\tau}d\tau + \int_0^\infty \left\langle a_Y(t)a_Y(t+\tau)\right\rangle e^{-i\omega_N\tau}d\tau$$

Our task is therefore reduced to computing these autocorrelation functions. They contain contributions from the stochastic dynamics of the electron magnetic dipole moment and from stochastic molecular rotation. Rewriting the matrix product in Equation (22) explicitly in terms of the Cartesian components of each matrix, we get:

$$\left\langle a_k(t)a_k(t+\tau)\right\rangle = \gamma_N^2\mu_0^2 \sum_{\alpha\beta\varepsilon\lambda} \left\langle r_{k\alpha}(t)d_{\alpha\beta}\mu_\beta(t)r_{k\varepsilon}(t+\tau)d_{\varepsilon\lambda}\mu_\lambda(t+\tau)\right\rangle \qquad (24)$$

where r_{ij} are elements of $\mathbf{R}$ and d_{ij} are elements of $\mathbf{D}$. If we assume that the dynamics of the electron magnetic moment is uncorrelated with molecular rotation, the average splits:

$$\left\langle a_k(t)a_k(t+\tau)\right\rangle = \gamma_N^2\mu_0^2 \sum_{\alpha\beta\varepsilon\lambda} d_{\alpha\beta}d_{\varepsilon\lambda} \left\langle r_{k\alpha}(t)r_{k\varepsilon}(t+\tau)\right\rangle\left\langle \mu_\beta(t)\mu_\lambda(t+\tau)\right\rangle \qquad (25)$$

The autocorrelation functions involving the elements of the rotation matrix are well known. It is reasonable to assume isotropic rotational diffusion here, in which case:

$$\left\langle r_{k\alpha}(t)r_{k\varepsilon}(t+\tau)\right\rangle = \frac{\delta_{\alpha\varepsilon}}{3}e^{-\tau/\tau_R} \qquad (26)$$

where τ_R is the rotational correlation time defined in Equation (16). Note that the right hand side does not depend on k, and that $\mathbf{D}$ is a symmetric matrix. This simplifies the sum:

$$\left\langle a_k(t)a_k(t+\tau)\right\rangle = \frac{\gamma_N^2\mu_0^2}{3}e^{-\tau/\tau_R} \sum_{\alpha\beta\lambda} d_{\lambda\alpha}d_{\alpha\beta} \left\langle \mu_\beta(t)\mu_\lambda(t+\tau)\right\rangle \qquad (27)$$

With this in place, our autocorrelation functions become:

$$\left\langle a_k(t)a_k(t+\tau)\right\rangle = \frac{\gamma_N^2\mu_0^2}{3}\mathrm{Tr}\left[\mathbf{D}^2\mathbf{G}(\tau)\right]e^{-\tau/\tau_R} \qquad (28)$$

where the autocorrelation tensor of the electron magnetic dipole vector is defined as:

$$\mathbf{G}(\tau) = \left\langle \vec{\mu}(t)\vec{\mu}^{\mathrm{T}}(t+\tau)\right\rangle \qquad (29)$$

All information about the dynamics of the electron magnetic dipole is now hidden inside $\mathbf{G}(\tau)$. After writing the dipolar matrix out explicitly, we find:

$$\left\langle a_k(t)a_k(t+\tau)\right\rangle = \frac{1}{3}\left(\frac{\mu_0}{4\pi}\right)^2\frac{\gamma_N^2}{r^6}\mathrm{Tr}\left[\left(3\hat{r}\cdot\hat{r}^{\mathrm{T}}-\mathbf{1}\right)^2\mathbf{G}(\tau)\right]e^{-\tau/\tau_R} \qquad (30)$$

where $\hat{r}$ is the unit vector pointing in the same direction as $\vec{r}$. After plugging this result back into Equation (23), we get the dipolar relaxation rate expressions:

$$R_1^{\text{dip}} = \frac{2}{3}\left(\frac{\mu_0}{4\pi}\right)^2 \frac{\gamma_N^2}{r^6} \text{Tr}\left[\left(3\hat{r}\cdot\hat{r}^{\text{T}} - \mathbf{1}\right)^2 \mathbf{G}(\omega_N)\right]$$

$$R_2^{\text{dip}} = \frac{1}{3}\left(\frac{\mu_0}{4\pi}\right)^2 \frac{\gamma_N^2}{r^6} \text{Tr}\left[\left(3\hat{r}\cdot\hat{r}^{\text{T}} - \mathbf{1}\right)^2 \left(\mathbf{G}(0) + \mathbf{G}(\omega_N)\right)\right]$$

(31)

Where $\mathbf{G}(\omega)$ is the spectral power density tensor that stores the statistics of both stochastic processes involved – the dynamics of the electron magnetic dipole and the molecular rotation:

$$\mathbf{G}(\omega) = \int_0^\infty \mathbf{G}(\tau) e^{-\tau/\tau_R} e^{-i\omega\tau} d\tau$$

(32)

This completes the derivation. If the unknown spectral density matrices are treated as fitting variables, the expressions in Equation (31) are remarkably simple compared to the prior art.[40,56,57] Because spectral power density is involved as a parameter, Equations (31) also have the advantage of being compatible with the multitude of sophisticated models of it (for example, pseudorotation[75]) that exist in the literature.[66] Fitting may be the best course of action though – in systems where non-rotational processes (*e.g.* transient solvent coordination) dominate ZFS fluctuations, the autocorrelation function in Equation (29) would be exceedingly hard to obtain from first principles.

2.6 Connection to electronic structure theory

Mathematical interpretations of $\mathbf{G}(\tau)$ and its Fourier transform $\mathbf{G}(\omega)$ are clear from Equation (29), but their physical meaning is less straightforward. In the special case when the stochastic perturbation in the electron momentum Hamiltonian is much weaker than the static part, the elements of the autocorrelation tensor in Equation (29) are

$$G_{nk}(\tau) = \left\langle \mu_n(t)\mu_k(t+\tau)\right\rangle =$$

$$= \text{Tr}\left[\hat{\rho}^{\text{eq}}\hat{\mu}_n \left\langle \exp_{(O)}\left(i\int_t^{t+\tau}\hat{\hat{H}}_E(t')dt'\right)\right\rangle \hat{\mu}_k\right]$$

(33)

where the Heisenberg picture is used, the indices n and k run over Cartesian coordinates, $\hat{\rho}^{\text{eq}}$ is the equilibrium electron density matrix, $\hat{\hat{H}}_E$ is the commutation superoperator of the electron Hamiltonian, and $\exp_{(O)}$ denotes a time-ordered exponential.

The average of the propagator is the subject of the very well developed theory of generalised cumulant expansions.[80,81] When the fluctuating part of the Hamiltonian is much smaller than the static part, GCE expansion to second order is identical to BRW theory,[59] therefore:

$$\left\langle \exp_{(O)}\left(i\int_t^{t+\tau}\hat{\hat{H}}_E(t')dt'\right)\right\rangle = \exp\left[i\hat{\hat{H}}_0\tau + \hat{\hat{R}}\tau\right]$$

(34)

where $\hat{\hat{H}}_0$ is the time average of $\hat{\hat{H}}_E(t)$ and $\hat{\hat{R}}$ is the negative-definite electron relaxation superoperator. The expression simplifies:

$$G_{nk}(\tau) = \text{Tr}\left[\hat{\rho}^{\text{eq}}\hat{\mu}_n \exp\left[i\hat{\hat{H}}_0\tau + \hat{\hat{R}}\tau\right]\hat{\mu}_k\right]$$

(35)

If we work in the eigenbasis of $\hat{H}_0$, the equilibrium density matrix $\hat{\rho}^{\text{eq}} = \exp\left(-\hat{H}_0/kT\right)$ is diagonal. For a single lanthanide, it is reasonable to neglect cross-relaxation processes, in which case the electron relaxation superoperator is also diagonal. Its action can then be reduced to an element-by-element Hadamard product $e^{\hat{R}\tau}\hat{\mu}_k = e^{\hat{R}\tau} \circ \hat{\mu}_k$. Writing the trace out explicitly, we obtain:

$$G_{nk}\left(\tau\right) = \sum_{pq} \rho_{pp}^{\text{eq}} \left\langle p\left|\hat{\mu}_n\right|q\right\rangle \left\langle q\left|\hat{\mu}_k\right|p\right\rangle e^{-\tau/\tau_{pq}} e^{-i\omega_{pq}\tau} \tag{36}$$

where ω_{pq} are energy differences between eigenstates of the static Hamiltonian, and $\tau_{pq} = \tau_{qp}$ is the characteristic time with which the element ρ_{pq} returns to its thermal equilibrium value. Taking the Fourier transform in Equation (32) we get

$$G_{nk}\left(\omega\right) = \text{Tr}\left[\hat{\rho}^{\text{eq}}\hat{\mu}_n\left[\hat{\mu}_k \circ \hat{j}\left(\omega\right)\right]\right] \tag{37}$$

where the components of the spectral power density matrix depend on the frequencies of the transitions and the corresponding relaxation times:

$$j_{pq}\left(\omega\right) = \frac{\tau_{\text{R},pq}}{1+\left(\omega+\omega_{pq}\right)^2 \tau_{\text{R},pq}^2}, \qquad \frac{1}{\tau_{\text{R},pq}} = \frac{1}{\tau_{\text{R}}} + \frac{1}{\tau_{pq}} \tag{38}$$

Technically, Equations (36)-(38) connect the formalism to the quantities that can be computed using electronic structure theory. In the limit of very fast electron relaxation, the ZFS and the Zeeman limits merge into the same expression (Section S1 of the Supplementary Information). However, it is unclear how well the diagonal approximation (*i.e.* the neglect of cross-relaxation processes) holds for the electron relaxation superoperator, or how to obtain its elements. We therefore recommend Equations (31) for practical data fitting and analysis.

3. Experimental results and discussion

The complexes we have studied experimentally are the next stage of our recent research into dual (relaxation, temperature) and triple (relaxation, temperature, pH) magnetic resonance imaging contrast agents.[11,12,15,16] Their synthesis and characterisation are described elsewhere.[17,21] The ligand is a derivative of 1,4,7,10-tetraazacyclododecane with a coordinated pyridyl group and triphosphinate donors, Ln=Tb, Dy, Ho, Er, Tm, Yb (Figure 2).
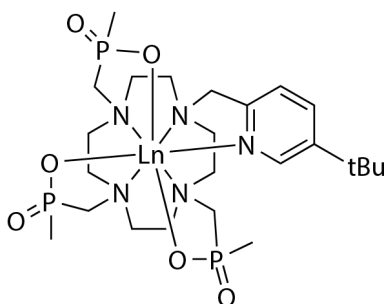

Figure 2. A schematic representation of the structure of the [LnL] complexes used in the experimental part of this work. Details of synthesis and characterisation are published elsewhere.[17,21]

The ligand contains a *tert*-butyl reporter group located about 6.6 Å away from the lanthanide, resonating up to 85 ppm away from the usual proton chemical shift range, and relaxing sufficiently quickly to allow rapid imaging. Recent studies show that the complexes are 8-coordinate and exist in solution mostly as a Λ-λλλλ twisted square antiprism isomer.[82]
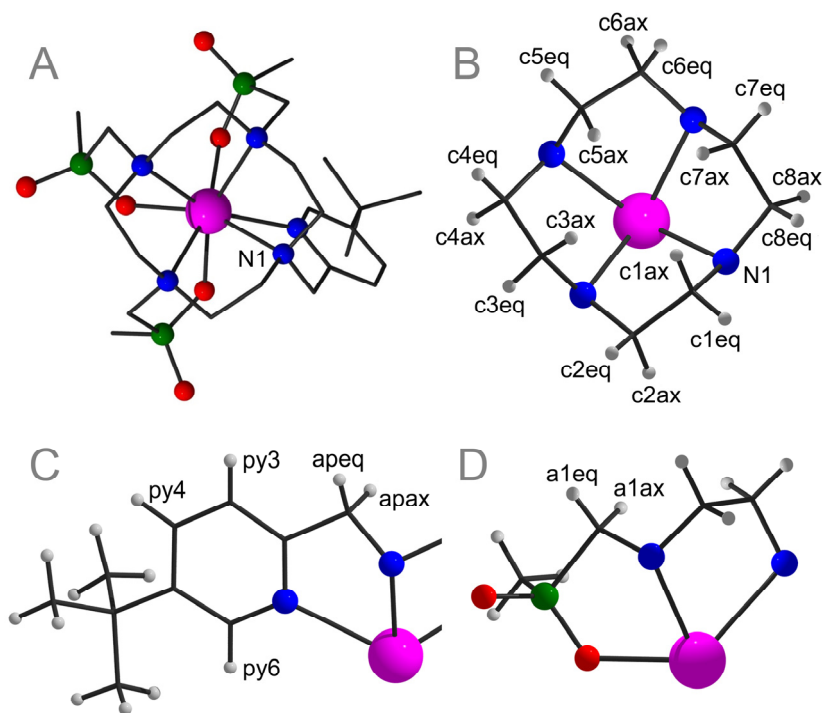

Figure 3. Relevant atom labels within the structure of [LnL]: (**A**) the X-ray structure of the Yb complex,[82] (**B**) a fragment of the same structure showing the axial (ax) and equatorial (eq) protons in the cyclen ring; (**C**) axial and equatorial protons with the ligand arm (ap), and within the pyridine ring (py); (**D**) axial and equatorial diastereotopic protons within the chelate ring formed by the ring nitrogen and the phosphinate oxygen.

In our previous work, we have assigned all proton NMR signals in [LnL] spectra and extracted the anisotropic part of the magnetic susceptibility tensor from pseudocontact shifts and DFT optimized structures.[21] Subsequent analysis of proton relaxation showed that the Solomon-Bloembergen-Morgan expressions in Equations (1) fail to reproduce the dependence of the relaxation rate on the proton position relative to the lanthanide (Figure 4).

The plots of the relaxation rate against r^{-6} indicate that it depends not only on the distance to the lanthanide, but also on the direction of the Ln-H vector. The relaxation rate also appears to depend on the sign of the magnetic anisotropy (and therefore pseudocontact shift): in the complexes with easy-plane anisotropy (Ln=Tb, Dy, Ho) the ligand arm protons tend to relax faster than the cyclen protons, and *vice versa* in the complexes with easy-axis magnetic anisotropy (Ln=Er, Tm, Yb).
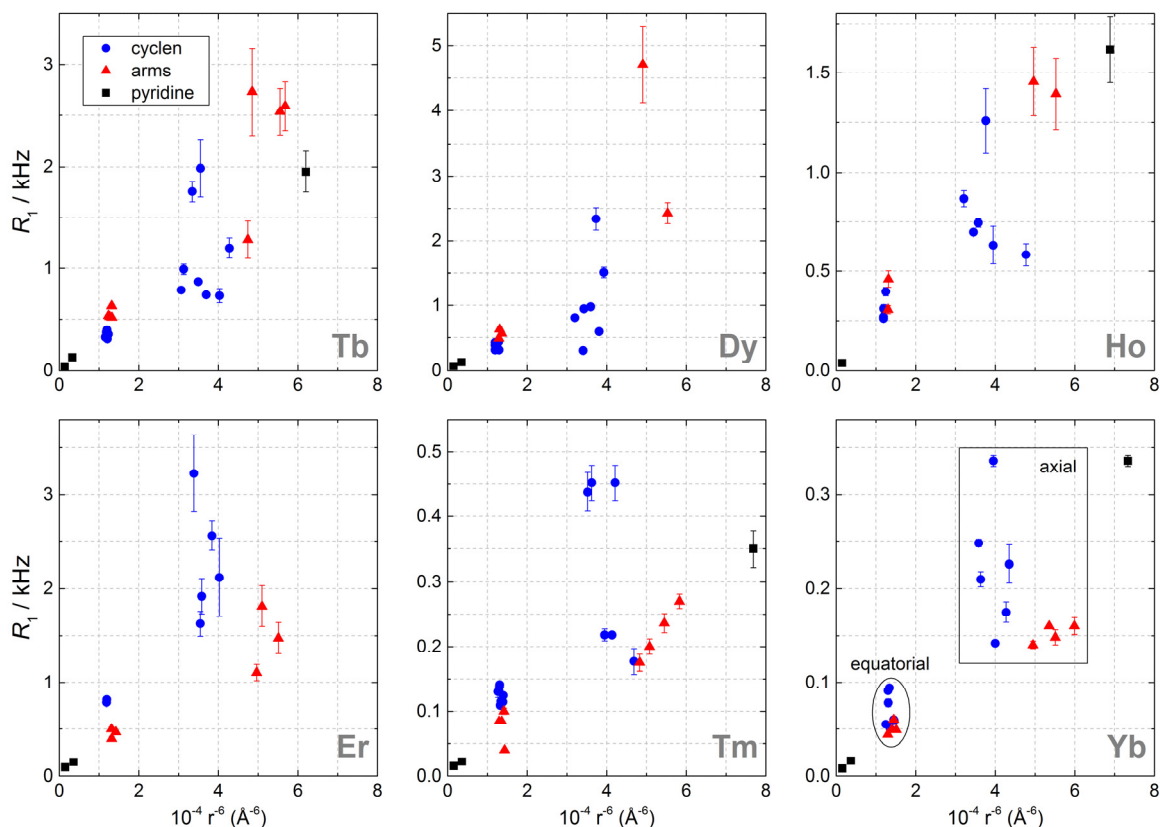

Figure 4. Proton longitudinal relaxation rates in isostructural [LnL] (Ln=Tb, Dy, Ho, Er, Tm, Yb) complexes, measured in D_2O at 300 K and 1.0 Tesla, and plotted against the inverse sixth power of Ln-H distance. Data points for cyclen protons are shown as blue circles, data for protons in the ligand arms as red triangles, and data for pyridine protons as black squares. The group highlighted in the Yb panel with rectangle contains axial protons with Ln-H distance of 3.4-3.7 Å; the group highlighted by the ellipse contains equatorial protons with Ln-H distance 4.2-4.4 Å. Point positions are similar in the other five plots. There are obvious deviations from the inverse sixth power distance dependence, which would be a straight line on these plots. Ligand arm protons tend to relax faster than cyclen protons in the complexes with easy-plane anisotropy (Ln= Tb, Dy, Ho) and *vice versa* in the complexes with easy-axis magnetic anisotropy (Ln=Er, Tm, Yb).

In the case of protons, we can neglect the relaxation contribution from the "native" diamagnetic chemical shielding tensor $\boldsymbol{\sigma}_0$ – its anisotropy is of the order of 10 ppm[83], much smaller than the contribution from the paramagnetic centre. The fact that Equations (17) depend on the square of the anisotropy makes it a very reasonable approximation: $\boldsymbol{\sigma}_0$ only contributes a few Hz to the kHz rates reported in Figure 4. We can therefore say that, for proton relaxation theory purposes, $\boldsymbol{\sigma} \approx -\mathbf{D} \cdot \boldsymbol{\chi}$. For most other nuclei, the contribution from $\boldsymbol{\sigma}_0$ would have to be included.
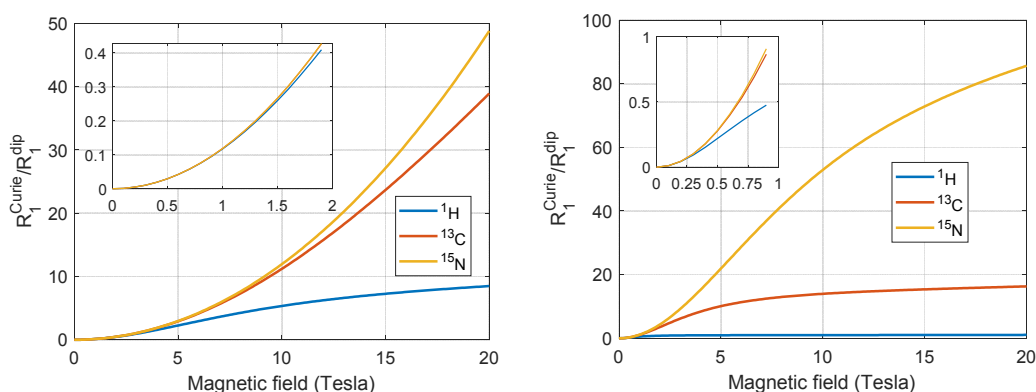
Figure 5. The ratio of Curie relaxation rate to the dipolar relaxation rate as a fuction of magnetic field computed for ^{1}H, ^{13}C and ^{15}N for a small molecule (left) with a rotational correlation time of 420 ps, and a protein (right) with τ_R=4 ns. Typical magnetic parameters for Tm(III) paramagnetic centers were used: τ_E=0.1 ns, μ_{eff}=7.5 Bohr magneton units.

Our measurements were carried out at 1.0 Tesla where the Curie relaxation rate is expected to be much smaller than the dipolar relaxation rate (Figure 5) , but it was included anyway – both the first and the second rank contribution in Equation (17). Paramagnetic chemical shielding tensors were estimated using the DFT optimized geometry, and the susceptibility tensor anisotropy was extracted using the PCS data published earlier.[21] The isotropic part of the susceptibility tensor was obtained from CASSCF calculations (0.8108, 0.9679, 0.9578, 0.7829, 0.4863, 0.1697 Å^3 for Tb, Dy, Ho, Er, Tm, Yb respectively) – see the Supplementary Information of our previous paper[17] for technical details of the CASSCF procedure. The rotational correlation time was obtained from the DFT geometry using the bead model[84] implemented in HYDRONMR[62] (η = 1.04 cP for D$_2$O at 27°C, resulting in τ_R = 420 ps). To avoid over-parameterisation, the small predicted Curie relaxation rate was fixed and only the six independent elements of $\mathbf{G}(\omega_N)$ in Equation (31) were varied using robust linear regression.
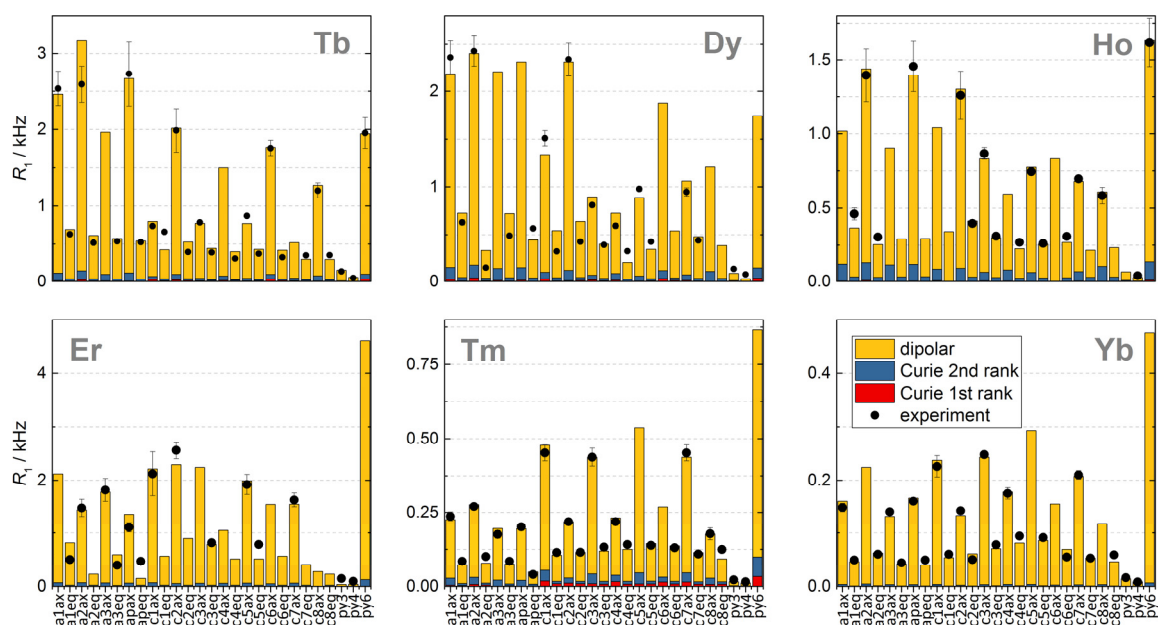

Figure 6. Analysis of proton longitudinal relaxation rates measured in D$_2$O at 300 K and 1.0 Tesla for [Ln.L] series (black circles). The computed Curie relaxation rates are shown in blue (second rank) and red (first rank); the dominant dipolar contribution is shown in yellow (see text for details).

The fitting results are shown in Figure 6. The Curie relaxation contribution at 1.0 Tesla is much smaller than the dipolar contribution, and the anisotropy in the longitudinal relaxation is chiefly due to the anisotropy of dipolar relaxation. This means, that at the field of 1.0 Tesla, we are in the "ZFS limit" discussed by Kowalewski[51-53] and Sharp.[40,56,57] This is further illustrated in Figure 7. *Ab initio* calculations suggest that the assumption of the ZFS limit for the systems in question is valid for all realistically available NMR magnets.

The fitting indicates that the anisotropic contribution to dipolar relaxation can reach 50% of the isotropic part. The obvious difference in the prediction quality between Figures 4 and 6 is a good illustration of the fact that relaxation anisotropy cannot be ignored.
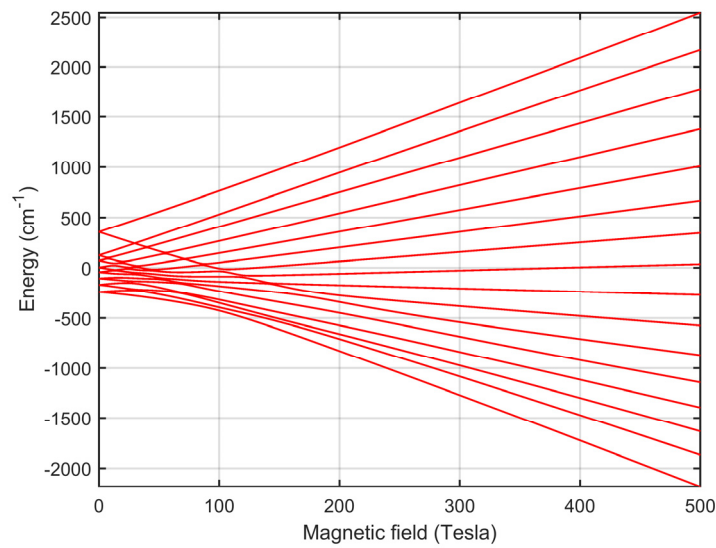

Figure 7. *Ab initio* simulation of the [DyL] energy levels splitting in the presence of the magnetic field (along z-axis in the molecular frame), computed using *Spinach*[85] (see the Supplementary Information for the source code and the ZFS Hamiltonian parameters obtained form a CASSCF calculation performed as described in our previous paper[17]). The Zeeman limit for the lowest energy level is reached only at very high magnetic field. ZFS is the dominant contribution up to 50 T.

The best fit components of the electron magnetic moment spectral power density matrix $\mathbf{G}(\omega_\mathrm{N})$ in Equation (31) are presented in Table 1, along with the standard error returned by the robust linear regression procedure. In the case of erbium, due to the small number of data points and large uncertainties, the standard linear regression was employed.

Table 1. The best-fit parameters of the electron magnetic moment spectral power density matrix components G_{nk} [$10^{-60}\mathrm{J}^2/\mathrm{T}^2\mathrm{s}$] and the corresponding standard errors extracted from the robust linear regression of R_1 data using Equation (31).

G_{nk}	Tb		Dy		Ho		Er		Tm		Yb	
	value	SE	value	SE	value	SE	value	SE	value	SE	value	SE
xx	1754	159	494	308	456	103	−915	563	−27	19	62	15
xy	−859	112	−1180	230	−640	62	−1010	558	−52	15	−25	13
xz	−207	126	451	267	98	106	−373	426	−105	21	−102	17
yy	2285	159	2696	289	913	211	2261	458	65	20	53	13
yz	−351	136	−30	256	−352	84	−1102	582	29	21	−8	14
zz	−196	136	518	185	800	103	2754	297	647	19	333	12

The spectral power density tensor extracted by fitting is strongly anisotropic. A notable observation is the expected 90° turn of the orientation of the eigenframe between Tb, Dy, Ho complexes and Er, Tm, Yb complexes. Unlike the axiality parameter of the susceptibility tensor, the axiality of $\mathbf{G}\left(\omega_{\mathrm{N}}\right)$ does not change sign when switching from easy-plane to easy-axis lanthanide systems.

Although the physical meaning of $\mathbf{G}\left(\omega_{\mathrm{N}}\right)$ is clear, it is unlikely that more detailed information (such as the ZFS tensor) can be extracted from it. As an order of magnitude estimate, we can say that $G_{\mathrm{iso}} \approx \tau_{\mathrm{E}} \chi_{\mathrm{iso}} kT / \mu_0$ – that would give us estimates for the electron relaxation time. Performing the calculations produces τ_{E} = 0.5, 0.4, 0.2, 0.5, 0.1 and 0.3 ps for Tb-Yb complexes respectively. These numbers are in surprisingly good agreement with the values known for similar isostructural series.[86] A more accurate determination of electron relaxation parameters from $\mathbf{G}\left(\omega_{\mathrm{N}}\right)$ would require the knowledge of the electronic structure theory energies and integrals that enter Equations (37) and (38). This is, in principle, possible – but would require a combination of CASSCF calculations and in-depth analysis of the statistics of stochastic ZFS fluctuations in lanthanide complexes in liquid state; this will be the subject of our next paper.

4. Conclusions and outlook

We have confirmed experimentally the long-standing theoretical suspicion that lanthanide-induced nuclear relaxation can be anisotropic in the molecular frame, and must be treated as such – any analysis based on the distance variation alone is at best a crude approximation for both the dipolar and the Curie mechanism. Except for Gd(III) complexes, any biomolecular structure refinement work using lanthanide spin tags must take this anisotropy into account, or risk significant errors. Prior work using "1/r⁶" models for lanthanides with a significant ZFS should be treated with appropriate caution.

The effects observed in this work go deeper than just a cross-correlation between the lanthanide magnetic susceptibility and the electron-nuclear dipolar interaction. Rather, they are the consequences of (a) zero-field splitting (ZFS) being greater than the Zeeman interaction[51-53], with the result that the electron magnetic moment is quantised in the ZFS eigenframe rather than along the magnet;[40,56,57] (b) the anisotropy of the magnetic susceptibility tensor being of the same order of magnitude as the isotropic part; (c) the product of the magnetic susceptibility tensor and the electron nuclear dipolar tensor having significant antisymmetric, as well as anisotropic, components.[37]

References

1. E. Ravera, G. Parigi, C. Luchinat, *J. Magn. Reson.*, 2017, **282**, 154-169.

2. I. Bertini, C. Luchinat, G. Parigi, E. Ravera, *NMR of Paramagnetic Molecules: Applications to Metallobiomolecules and Models*, Elsevier, 2016.

3. P. Caravan, J. J. Ellison, T. J. McMurry, R. B. Lauffer, *Chem. Rev.*, 1999, **99**, 2293-2352.

4. G. M. Clore, C. Tang, J. Iwahara, *Curr. Op. Struct. Biol.*, 2007, **17**, 603-616.

5. T. Maly, G. T. Debelouchina, V. S. Bajaj, K.-N. Hu, C.-G. Joo, M. L. Mak-Jurkauskas, J. R. Sirigiri, P. C. van der Wel, J. Herzfeld, R. J. Temkin, *J. Chem. Phys.*, 2008, **128**, 02B611.

6. C. Laustsen, T. S. Nørlinger, D. C. Hansen, H. Qi, P. M. Nielsen, L. B. Bertelsen, J. H. Ardenkjaer-Larsen, H. S. Jørgensen, *Magn. Reson. Med.*, 2016, **75**, 515-518.

7. I. Park, C. von Morze, J. M. Lupo, J. H. Ardenkjaer-Larsen, A. Kadambi, D. B. Vigneron, S. J. Nelson, *Magn. Reson. Med.*, 2016.

8. G. Otting, *Ann. Rev. Biophys.*, 2010, **39**, 387-405.

9. P. Caravan, *Acc. Chem. Res.*, 2009, **42**, 851-862.

10. G. M. Clore, J. Iwahara, *Chem. Rev.*, 2009, **109**, 4108-4139.

11. A. M. Kenwright, I. Kuprov, E. De Luca, D. Parker, S. U. Pandya, P. K. Senanayake, D. G. Smith, *Chem. Comm.*, 2008, 2514-2516.

12. K. L. N. Finney, A. C. Harnden, N. J. Rogers, P. K. Senanayake, A. M. Blamire, D. O'Hogain, D. Parker, *Chem. Eur. J.*, 2017, **23**, 7976-7989.

13. D. Coman, R. A. Graaf, D. L. Rothman, F. Hyder, *NMR Biomed.*, 2013, **26**, 1589-1595.

14. P. Harvey, A. M. Blamire, J. I. Wilson, K.-L. N. Finney, A. M. Funk, P. K. Senanayake, D. Parker, *Chem. Sci.*, 2013, **4**, 4251-4258.

15. P. K. Senanayake, N. J. Rogers, K.-L. N. A. Finney, P. Harvey, A. M. Funk, J. I. Wilson, D. O'Hogain, R. Maxwell, D. Parker, A. M. Blamire, *Magn. Reson. Med.*, 2017, **77**, 1307-1317.

16. K. H. Chalmers, E. De Luca, N. H. Hogg, A. M. Kenwright, I. Kuprov, D. Parker, M. Botta, J. I. Wilson, A. M. Blamire, *Chem. Eur. J.*, 2010, **16**, 134-148.

17. M. Vonci, K. Mason, E. A. Suturina, A. T. Frawley, S. G. Worswick, I. Kuprov, D. Parker, E. J. McInnes, N. F. Chilton, *J. Am. Chem. Soc.*, 2017, **139**, 14166-14172.

18. A. M. Funk, K.-L. N. Finney, P. Harvey, A. M. Kenwright, E. R. Neil, N. J. Rogers, P. K. Senanayake, D. Parker, *Chem. Sci.*, 2015, **6**, 1655-1662.

19. A. M. Funk, P. Harvey, K.-L. N. Finney, M. A. Fox, A. M. Kenwright, N. J. Rogers, P. K. Senanayake, D. Parker, *Phys. Chem. Chem. Phys.*, 2015, **17**, 16507-16511.

20. N. J. Rogers, K.-L. N. Finney, P. K. Senanayake, D. Parker, *Phys. Chem. Chem. Phys.*, 2016, **18**, 4370-4375.

21. E. A. Suturina, K. Mason, C. F. G. C. Geraldes, I. Kuprov, D. Parker, *Angew. Chem. Intl. Ed.*, 2017, **56**, 12215-12218.

22. B. Bleaney, *J. Magn. Reson.*, 1972, **8**, 91-100.

23. I. Solomon, *Phys. Rev.*, 1955, **99**, 559.

24. N. Bloembergen, *J. Chem. Phys.*, 1957, **27**, 572-573.

25. N. Bloembergen, L. Morgan, *J. Chem. Phys.*, 1961, **34**, 842-850.

26. M. Gueron, *J. Magn. Reson.*, 1975, **19**, 58-66.

27. I. Bertini, C. Luchinat, *NMR of paramagnetic molecules in biological systems*, Benjamin Cummings Publishing Company, 1986.

28. I. Bertini, C. Luchinat, G. Parigi, *Solution NMR of paramagnetic molecules: applications to metallobiomolecules and models*, Elsevier, 2001.

29. M. Goldman, *J. Magn. Reson.*, 1984, **60**, 437-452.

30. I. Burghardt, R. Konrat, G. Bodenhausen, *Mol. Phys.*, 1992, **75**, 467-486.

31.   R. Konrat, H. Sterk, *Chem. Phys. Lett.*, 1993, **203**, 75-80.

32.   R. Ghose, J. H. Prestegard, *J. Magn. Reson.*, 1997, **128**, 138-143.

33.   A. Kumar, R. C. R. Grace, P. Madhu, *Progr. NMR Spec.*, 2000, **37**, 191-319.

34.   I. Bertini, J. Kowalewski, C. Luchinat, G. Parigi, *J. Magn. Reson.*, 2001, **152**, 103-108.

35.   G. Pintacuda, A. Kaikkonen, G. Otting, *J. Magn. Reson.*, 2004, **171**, 233-243.

36.   H. W. Orton, I. Kuprov, C.-T. Loh, G. Otting, *J. Phys. Chem. Lett.*, 2016, **7**, 4815-4818.

37.   A. J. Vega, D. Fiat, *Mol. Phys.*, 1976, **31**, 347-355.

38.   J. Kowalewski, L. Nordenskiöld, N. Benetis, P.-O. Westlund, *Progr. NMR Spec.*, 1985, **17**, 141-185.

39.   J. A. Peters, J. Huskens, D. J. Raber, *Progr. NMR Spec.*, 1996, **28**, 283-350.

40.   R. Sharp, L. Lohr, J. Miller, *Progr. NMR Spec.*, 2001, **38**, 115-158.

41.   J. Kowalewski, C. Luchinat, T. Nilsson, G. Parigi, *J. Phys. Chem. A*, 2002, **106**, 7376-7382.

42.   L. Helm, *Progr. NMR Spec.*, 2006, **49**, 45-64.

43.   M. Goldman, *J. Magn. Reson.*, 2001, **149**, 160-187.

44.   A. G. Redfield, *IBM J. Res. Dev.*, 1957, **1**, 19-31.

45.   R. K. Wangsness, F. Bloch, *Phys. Rev.*, 1953, **89**, 728.

46.   G. Moro, J. H. Freed, *J. Phys. Chem.*, 1980, **84**, 2837-2840.

47.   G. Moro, J. H. Freed, *J. Chem. Phys.*, 1981, **74**, 3757-3773.

48.   R. Kubo, *Hyperf. Inter.*, 1981, **8**, 731-738.

49.   G. Pintacuda, G. Otting, *J. Am. Chem. Soc.*, 2002, **124**, 372-373.

50.   M. John, G. Pintacuda, A. Y. Park, N. E. Dixon, G. Otting, *J. Am. Chem. Soc.*, 2006, **128**, 12910-12916.

51.   N. Benetis, J. Kowalewski, L. Nordenskiöld, H. Wennerström, P.-O. Westlund, *Mol. Phys.*, 1983, **48**, 329-346.

52.   N. Benetis, J. Kowalewski, L. Nordenskiöld, H. Wennerström, P.-O. Westlund, *J. Magn. Reson.*, 1984, **58**, 261-281.

53.   N. Benetis, J. Kowalewski, *J. Magn. Reson.*, 1985, **65**, 13-33.

54.   R. A. Layfield, M. Murugesu, *Lanthanides and Actinides in Molecular Magnetism*, Wiley, 2015.

55.   L. Sorace, C. Benelli, D. Gatteschi, *Chemical Society Reviews*, 2011, **40**, 3092-3104.

56.   R. R. Sharp, *J. Chem. Phys.*, 1990, **93**, 6921-6928.

57.   N. Schaefle, R. Sharp, *J. Magn. Reson.*, 2005, **176**, 160-170.

58.   J. Blicharski, *Zeitschr. Naturforsch. A*, 1972, **27**, 1456.

59.   I. Kuprov, *J. Magn. Reson.*, 2011, **209**, 31-38.

60.   I. Kuprov, N. Wagner-Rundell, P. J. Hore, *J. Magn. Reson.*, 2007, **184**, 196-206.

61.   S. Szymanski, A. M. Gryff-Keller, G. Binsch, *J. Magn. Reson.*, 1986, **68**, 399-432.

62.   J. G. De la Torre, M. Huertas, B. Carrasco, *J. Magn. Reson.*, 2000, **147**, 138-146.

63.   R. Paquin, P. Pelupessy, L. Duma, C. Gervais, G. Bodenhausen, *J. Chem. Phys.*, 2010, **133**, 034506.

64.   A. Biternas, G. Charnock, I. Kuprov, *J. Magn. Reson.*, 2014, **240**, 124-131.

65.   M. Siemens, J. Hancock, D. Siminovitch, *Solid State Nuclear Magnetic Resonance*, 2007, **31**, 35-54.

66.   J. Kowalewski, D. Kruk, G. Parigi, *Adv. Inorg. Chem.*, 2005, **57**, 41-104.

67.   H. Sternlicht, *J. Chem. Phys.*, 1965, **42**, 2250-2251.

68.   S. H. Konig, *J. Magn. Reson.*, 1982, **47**, 441-453.

69.   P. L. Nordio, U. Segre, *J. Magn. Reson.*, 1977, **27**, 465-473.

70. I. Bertini, C. Luchinat, M. Mancini, G. Spina, *J. Magn. Reson.*, 1984, **59**, 213-222.

71. I. Bertini, C. Luchinat, K. V. Vasavada, *J. Magn. Reson.*, 1990, **89**, 243-254.

72. I. Bertini, C. Luchinat, J. Kowalewski, *J. Magn. Reson.*, 1985, **62**, 235-241.

73. I. Bertini, O. Galas, C. Luchinat, G. Parigi, *J. Magn. Reson.*, 1995, **113**, 151-158.

74. I. Bertini, F. Capozzi, C. Luchinat, G. Nicastro, Z. Xia, *J. Phys. Chem.*, 1993, **97**, 6351-6354.

75. D. Kruk, T. Nilsson, J. Kowalewski, *Phys. Chem. Chem. Phys.*, 2001, **3**, 4907-4917.

76. E. Belorizky, P. H. Fries, L. Helm, J. Kowalewski, D. Kruk, R. R. Sharp, P.-O. Westlund, *J. Chem. Phys.*, 2008, **128**, 052315.

77. B. Halle, *J. Chem. Phys.*, 2009, **131**, 224507.

78. A. Carrington, G. Luckhurst, *Mol. Phys.*, 1964, **8**, 125-132.

79. B. M. Alsaadi, F. J. Rossotti, R. J. Williams, *J. Chem. Soc. Dalton Trans.*, 1980, 2147-2150.

80. R. Kubo, *J. Phys. Soc. Japan*, 1962, **17**, 1100-1120.

81. J. H. Freed, *J. Chem. Phys.*, 1968, **49**, 376-391.

82. K. Mason, N. J. Rogers, E. A. Suturina, I. Kuprov, J. A. Aguilar, A. S. Batsanov, D. S. Yufit, D. Parker, *Inorg. Chem.*, 2017, **56**, 4028-4038.

83. D. Sitkoff, D. A. Case, *Progr. NMR Spec.*, 1998, **32**, 165-190.

84. V. Bloomfield, W. Dalton, K. Van Holde, *Biopolymers*, 1967, **5**, 135-148.

85. H. Hogben, M. Krzystyniak, G. Charnock, P. Hore, I. Kuprov, *J. Magn. Reson.*, 2011, **208**, 179-194.

86. A. M. Funk, P. H. Fries, P. Harvey, A. M. Kenwright, D. Parker, *J. Phys. Chem. A*, 2013, **117**, 905-917.